Journal of Hazardous Materials 174 (2010) 84–92

Contents lists available at ScienceDirect

Journal of Hazardous Materials

journal homepage: www.elsevier.com/locate/jhazmat

Brazil nut shells as a new biosorbent to remove methylene blue and indigo carmine from aqueous solutions

Suzana Modesto de Oliveira Brito[a,*], Heloysa Martins Carvalho Andrade[b], Luciana Frota Soares[a], Rafael Pires de Azevedo[a]

[a] Departamento de Ciências Exatas, Universidade Estadual de Feira de Santana – UEFS, Av. Transnordestina s/n, Novo Horizonte, 44036-900 Feira de Santana, Bahia, Brazil
[b] Instituto de Química, Universidade Federal da Bahia – UFBA, End: Rua Barão de, Jeremoabo, s/n - Campus Universitário de Ondina, 40170-115 Salvador, Bahia, Brazil

ARTICLE INFO

Article history:
Received 10 June 2009
Received in revised form 3 September 2009
Accepted 6 September 2009
Available online 11 September 2009

Keywords:
Biosorption
Low-cost adsorbents
Dye adsorption
Wastewater treatment
Color removal

ABSTRACT

The adsorption of methylene blue and indigo carmine, respectively a basic and an acid dye, was studied on raw Brazil nut shells. The dye removal from solution by BNS was governed by: (i) polarization effects between the colored ions and the surface sites, leading to physisorbed species due to weak electrostatic forces and (ii) diffusion limitations affecting the kinetic parameters. Thermodynamic studies showed that the adsorption of methylene blue and of indigo carmine was spontaneous and exothermic occurring with entropy decrease. H^0 values confirmed the physical nature of the adsorption processes. The adsorption followed the Langmuir model and pseudo-second order kinetics over the entire range of tested concentrations but the process was controlled by intraparticle diffusion. The maximal uptakes were 7.81 mg g^{-1}, for methylene blue, and 1.09 mg g^{-1} for indigo carmine, at room temperature. These results indicate that Brazil nut shells may be useful as adsorbent either for basic or acid dyes.

1. Introduction

Dye residues are aesthetically unpleasant and interfere with the transmission of light necessary to photosynthesis, causing disturbance in the ecological systems of the receiving waters. The dyestuffs are very difficult to decompose and the conventional methods such as coagulation, photodegradation, ozonation and adsorption, although widely used, are not efficient for all effluents or dyes [1–5]. These methods are expensive (activated carbon adsorption), produce concentrated sludges (Fenton's reagent treatment) or are inadequate to treat large volumes of effluent without the risk of clogging (membrane filtration) [5].

The adsorption processes give the best results as they can be used to remove different types of coloring materials, providing an attractive treatment, especially if "low-cost" adsorbents are available. According to Bailey et al. [6], a low-cost adsorbent requires little processing, is abundant in nature or is a byproduct or waste material from another industry. Several non-conventional sorbents have been investigated including banana pith [7,8], coir pith [9,10], bagasse pith [11], corn cob [12], sawdust [13], apple pomace [14], date pits [15], peat [16,17], fruit peel [18,19], rice husk ash [20], spent tea leaves [21], etc. Nigam et al. [22] reported that the degradation of dyes occurred in a few weeks by solid state fermentation of dye adsorbed residues in the presence of fungi and that the protein content was increased in the presence of fungal biomass [5]. In this way, provided an appreciable extension of fungal colonies, the fermented substrate could be useful as soil fertilizer, avoiding extra costs of regeneration or disposal of dye saturated biomass biosorbent.

Brazil nut (*Berthollitia excelsa* H.B.K.) is found throughout the Amazon rain forest and the annual production in 2007 was 30 000 tons [23] and this production generates a huge amount of shells as waste material. In this work, Brazil nut shells (BNS) were investigated as biosorbent to remove methylene blue (MB) and indigo carmine (IC) from aqueous solutions. MB is used in different fields, such as medicine and chemistry [24,25], and has been used as model molecule in a great number of adsorption and photocatalysis studies for environmental purposes. IC is one of the synthetic indigo dyes and is used as a colorant for food, pharmaceuticals and cosmetics [26,27]. MB and IC are, respectively, basic and acid dye molecules and therefore release negative and positive charged colored moieties in aqueous solution, allowing the assessment of any preferential surface interaction. The chemical structures of these dyes are shown in Fig. 1(a) and (b).

* Corresponding author. Tel.: +55 752248086; fax: +55 752248086.
E-mail address: smobrito@uefs.br (S.M. de Oliveira Brito).

0304-3894/$ – see front matter © 2009 Elsevier B.V. All rights reserved.
doi:10.1016/j.jhazmat.2009.09.020

Nomenclature

BNS	Brazil nut shells
MB	methylene blue
IC	indigo carmine
SEM	scanning electron microscopy
PZC	point of zero charge
pH_{PZC}	pH of the point of zero charge
ΔH^0	standard enthalpy of adsorption
ΔS^0	standard entropy of adsorption
ΔG^0	Gibbs free energy of adsorption
K_C	equilibrium constant of adsorption
R	gas constant 8.314472 J K^{-1} mol^{-1}
C_{ads}	concentration of adsorbed dye
C_e	equilibrium concentration (mg L^{-1})
Q_e	amount of adsorbed dye per mass of adsorbent at equilibrium (mg g^{-1})
Q_t	amount of adsorbed dye at time t (mg g^{-1})
k_{ad}	pseudo-first order rate constant (min^{-1})
k_2 or K_a	pseudo-second order rate constant (g mg^{-1} min^{-1})
E_a	activation energy (J mol^{-1})
Q_{max}	Langmuir monolayer capacity (mg g^{-1})
K_L	Langmuir constant (L mg^{-1})
K_F	Freundlich constant (L mg^{-1})
n	Freundlich heterogeneity factor

2. Materials and methods

2.1. Chemicals and samples

The BNS samples were crushed, washed with distilled water and dried in an oven at 105 °C for 24 h. The dry material was sieved into the following particle size ranges: >710 μm, 710–500 μm and <500 μm. The samples were stored in closed bottles to be used in the adsorption studies without any further pre-treatment in order to avoid extra costs. The density of dry BNS was 0.63 g L^{-1}.

MB (MM = 319.85 g mol^{-1}) was supplied by Cinética Química Ltda. and IC (MM = 466.36 g mol^{-1}) was purchased from Vetec Química Ltda. Aqueous solutions of the dyes were prepared using deionized water.

2.2. Characterization of the biosorbent

2.2.1. Scanning electron microscopy images

SEM images were collected in a Carl Zeis LEO 1430 VP equipment using aluminum stubs with adhesive carbon tape with the BNS powder covered with gold for best results.

2.2.2. pH of BNS suspensions

The pH of adsorbent suspension was measured to investigate changes in pH due to any soluble species released from the natural material in water. The procedure was the same of Al-Degs et al. [3]. The samples were shaken in distilled water (10% (w/v) mixture) for 3 h and then the pH was measured in a MARTE MB-10 potentiometer with a glass electrode.

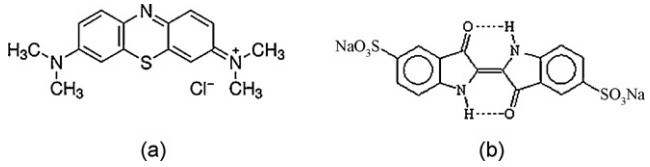

Fig. 1. Chemical structures of (a) methylene blue (MB) and (b) indigo carmine (IC).

2.2.3. Studies on BNS surface acidity and basicity

The surface acidity studies were performed in accordance to Al-Degs et al. [3]. Before testing, the BNS powder was washed with distilled water and dried at 100 °C for 24 h. Triplicate samples (0.5 g) were shaken in 50 mL of 0.0100 mol L^{-1} sodium hydroxide solution for 24 h, at room temperature. Thereafter, the samples were filtered and the remaining NaOH was titred with 0.0100 mol L^{-1} HCl solution in a MARTE MB-10 potentiometer with a glass electrode.

The surface basicity was determined in a similar way, using a 0.0100 mol L^{-1} HCl solution. The remaining acid was titred with NaOH. The results were expresses in mmol H^+ or OH^- per gram of BNS.

2.2.4. Point of zero charge

The point of zero charge (PZC) of BNS was determined by the solid addition method, as described by Vieira et al. [28]. Eight vials containing solutions of pH in the range of 3–10 (pH_0) and 0.10 g of BNS were shaken for 24 h at room temperature and the final pH was measured with a MARTE MB-10 potentiometer and a glass electrode. The difference between the initial and final pH (ΔpH) was plotted against the initial pH (pH_0) and the point where ΔpH = 0 was taken as the point of zero charge.

2.3. Effect of solution pH on adsorption

In order to study the effect of pH on dye adsorption, the pH of the solutions was varied from 3 to 10, by adding 0.1 M NaOH or 0.1 M HCl solutions. The batch procedure at each pH was followed as above described using an initial concentration of 1100 mg L^{-1}. The pH of the solutions during adsorption was monitored using a MARTE MB-10 potentiometer with a glass electrode.

2.4. Batch and kinetic studies

In order to evaluate the feasibility of adsorption, laboratory batch studies were carried out using 100-mL conical flasks containing 25 mL of the test solutions at the desired initial dye concentration. A previously defined amount of the adsorbent material (BNS) was then added and the flasks were shaken at room temperature, for different contact times. After filtration through filter paper the solution dye concentration was determined using a Femto 700 Plus UV/VIS spectrophotometer at 660 nm and 610 nm for MB and IC, respectively.

Blank tests were conducted in two ways: (i) without adsorbent, to check for the retention of the dye at the filter paper surface and other possible losses, and (ii) without the dye (in pure water), to verify if any colored species present in the shells were water soluble and would contribute to the color of water, masking in the results.

Dye losses at the filter paper surface were negligible and no significant color effect could be accounted to the BNS adsorbent.

The maximum contact time (equilibrium) was established in appropriate tests and for the isotherms it was taken as 120 min. The initial concentration of dyes varied from 100 mg L^{-1} to 1500 mg L^{-1}. The amount of adsorbent used was arbitrarily taken as 2.5 g.

Unless when otherwise indicated, the experiments were carried at pH = 6.50 which corresponded to the initial pH of both dye solutions.

2.5. Effect of particle size

In order to study the effect of particle size on adsorption, batch experiments as above described were carried out using the BNS fractions >710 μm, 710–500 μm and <500 μm and an initial dye concentration of 1100 mg L^{-1}, at room temperature.

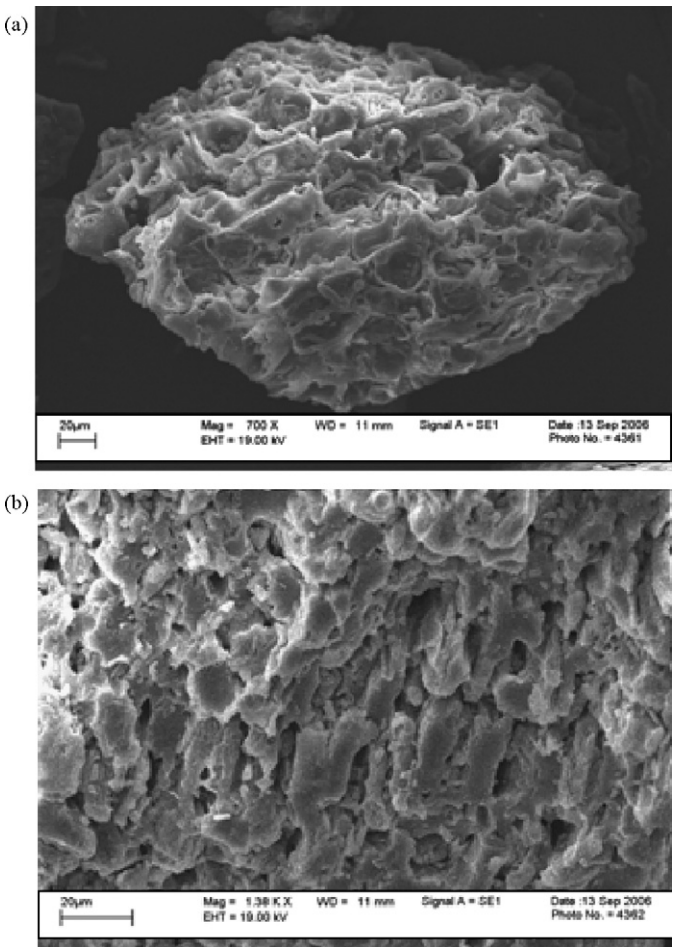

Fig. 2. SEM images of BNS showing (a) a particle and (b) the cavities of the material.

2.6. Effect of temperature

The effect of temperature on the adsorption was investigated in the range 293–333 K (20–60 °C) in batch experiments already described and initial concentration of 1100 mg L^{-1}.

3. Results and discussion

3.1. Scanning electron microscopy images

The SEM images of BNS particles are shown in Fig. 2. The mean size of surface cavities was measured on the image and the average diameter was 7 μm. These cavities are large enough to allow the molecules of dyes to penetrate into the lignocellulosic structure and interact therein with the surface groups.

3.2. pH of BNS suspension and surface acid–base properties

The pH of BNS aqueous suspension corresponded to that of the deionized water (pH = 6.50), even after 3 h under stirring. This indicates that the adsorbent does not introduce acid or basic species to the solution. Additionally, the pH of the dye solutions did not vary during the adsorption procedure, maintaining the initial value adjusted either with HCl or NaOH. These results suggest that ion exchange does not occur between the BNS surface and the aqueous solution.

The amount of surface acid and basic sites was determined by the previously described titration method and results corresponded to 7.24 mmol H^+/g and 2.20 mmol OH^-/g respectively.

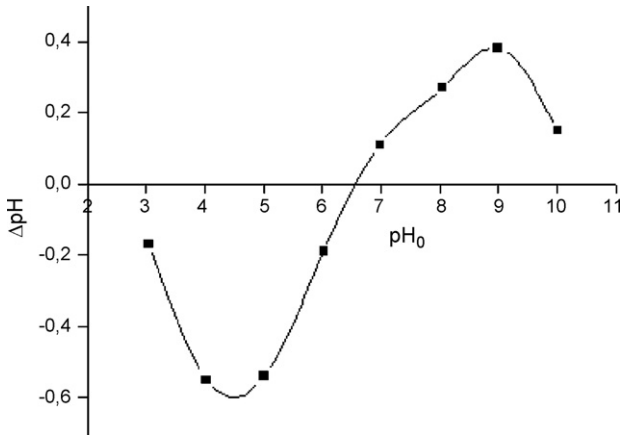

Fig. 3. Point of zero charge of BNS.

These figures indicate that the surface is mostly acidic. Accordingly, it could be expected that the adsorption of negatively charged species should be favored, namely the adsorption of the colored anionic IC moiety should be preferential in detriment of the colored cationic MB moiety.

Nevertheless, as shown in Fig. 3, the pH_{PZC} of BNS was determined to be 6.57. Therefore, at a solution pH > 6.57, the BNS surface is negatively charged and the adsorption of MB^+ moieties is favorable while at pH < 6.57 the BNS surface becomes positively charged and then the adsorption of IC^- moieties is favorable. In order to compare the adsorption properties of BNS toward acid and basic dyes, the experiments were carried out at pH = pH_{PZC}, corresponding to a nearly neutral surface.

3.3. Effect of adsorption pH

In order to confirm these last assumptions, the pH effects were investigated and the results are shown in Fig. 4. As expected, the percentage of MB removal increased with the increase of solution pH as the surface becomes progressively more negatively charged. Nevertheless, the MB removal was nearly constant in the pH range of 7.0–10.0, suggesting the BNS adsorption was attained.

Contrarily, the adsorption of indigo carmine was not affected by pH, over the entire studied range. This unexpected behavior suggests that diffusion limitations could affect the adsorption of the heavier anionic dye onto the BNS surface.

Consequently, these findings suggest that the dye removal from solution by BNS could be governed by: (i) polarization effects between the colored ions and the surface sites, leading to physisorbed species due to weak electrostatic forces, and (ii) diffusion limitations affecting the kinetic parameters, namely mass transfer of the dye molecules into the porous structure of the biosorbent.

3.4. Effect of temperature

Fig. 5 shows the effect of temperature on the adsorption of MB and IC on BNS, in the range of 293–333 K (20–60 °C). The amount of adsorbed dye decreased with the increase of temperature, as expected for an exothermic adsorption process. The set of thermodynamic parameters, enthalpy (ΔH^0), entropy (ΔS^0), Gibbs free energy (ΔG^0) and equilibrium constant (K_C), were determined for the MB-BNS and IC-BNS systems, using Eqs. (1)–(3) [29]:

$$\log K_C = -\frac{\Delta H^0}{2.303RT} + \frac{\Delta S^0}{2.303R} \quad (1)$$

$$\Delta G^0 = -RT \ln(K_C) \quad (2)$$

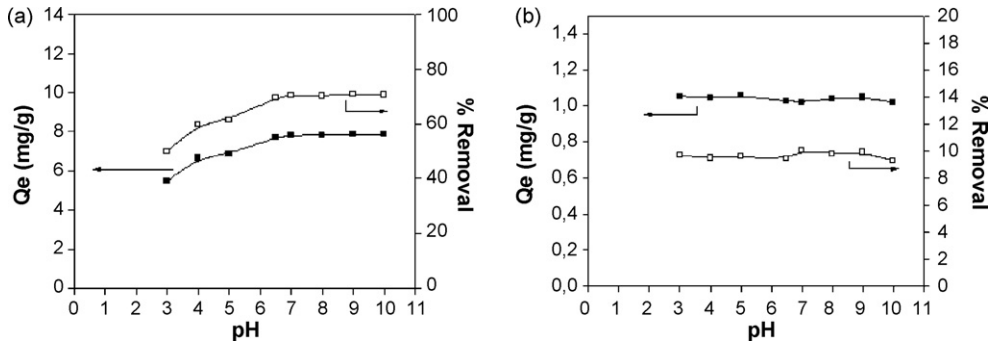

Fig. 4. Influence of pH on the adsorption capacity of (a) MB and (b) IC on BNS. C_i = 1100 mg L^{-1}, T = 303 K, and t = 120 min.

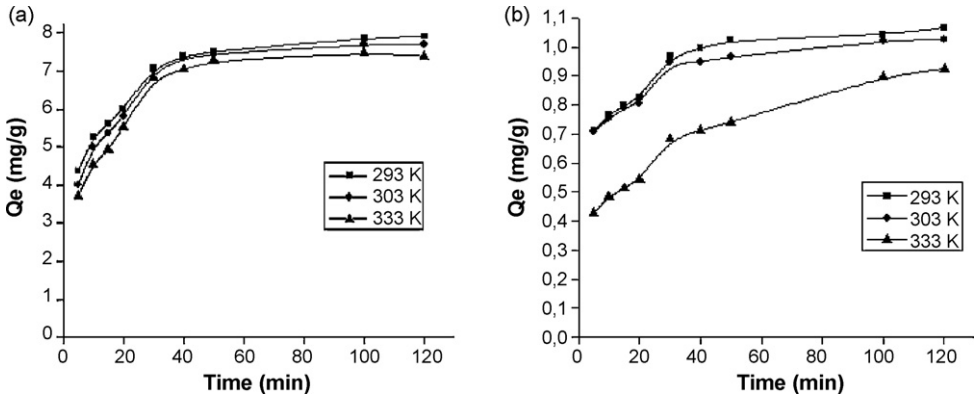

Fig. 5. Effect of temperature on adsorption of (a) MB and (b) IC onto BNS. C_i = 1100 mg L^{-1}, pH = 6.50, and t = 120 min.

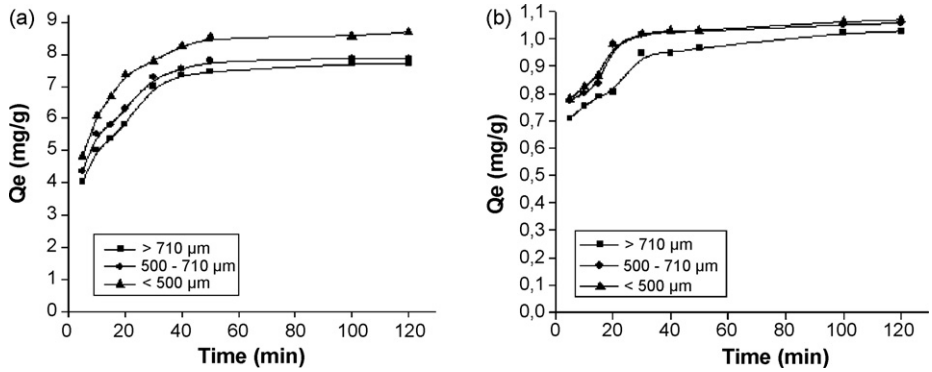

Fig. 6. Influence of particle size on the adsorption of (a) MB and (b) IC over BNS. C_i = 1100 mg L^{-1}, T = 303 K, pH = 6.50, and t = 120 min.

Table 1
Thermodynamic properties of adsorption of MB on BNS.

T (K)	K_c	ΔH^0 (kJ mol^{-1})	ΔS^0 (J/K mol)	R^2	ΔG^0 (kJ mol^{-1})	% dye removal
293	2.54	−5.22	−112.23	0.999	−2.27	71.77
303	2.29				−2.09	69.61
333	2.04				−1.97	67.07

Table 2
Thermodynamic properties of adsorption of IC on BNS.

T (K)	K_c	ΔH^0 (kJ mol^{-1})	ΔS^0 (J/K mol)	R^2	ΔG^0 (kJ mol^{-1})	% dye removal
293	0.11	−3.20	−29.39	0.998	−5.42	9.75
303	0.10				−5.71	9.40
333	0.09				−6.60	8.45

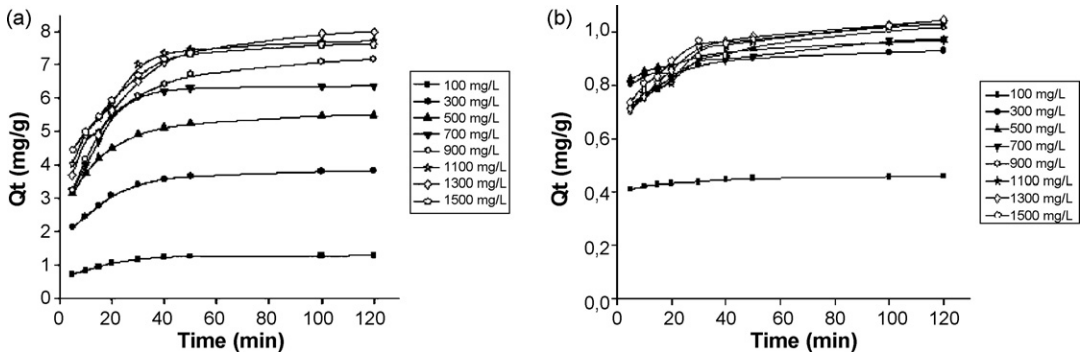

Fig. 7. Effect of contact time on the uptake of (a) MB and (b) IC on BNS at different initial concentrations and pH = 6.5 and 303 K.

$$K_C = \frac{C_{ads}}{C_e} \quad (3)$$

The values of the thermodynamic parameters for the adsorption of MB and IC onto BNS are respectively collected in Tables 1 and 2 and indicate that the adsorption processes are spontaneous and exothermic, involving entropy decrease. In addition, these values further confirm some of the assumptions previously discussed in this work. Thus, the values of ΔG^0, ranging from -1.97 to $-6.60\,kJ\,mol^{-1}$ are consistent with electrostatic interactions between the surface sites [30] and the charged adsorbates, while the small and negative ΔH^0 values, namely -5.22 and $-3.20\,kJ\,mol^{-1}$ for MB and IC respectively, further confirm the physical nature of the adsorption processes, involving weak attractive forces [31,32].

3.5. Effect of particle size

Although finer particles have been reported in most adsorption studies [10,18,28,31] larger particles have been used [11,16] and seem to be more advantageous for practical uses due to reduced costs of grinding and easier recovery of the saturated biosorbent. Fig. 6 shows the influence of the particle size on the adsorption of MB and IC onto BNS. No significant change was observed in the particle size range $500\,\mu m < d_p < 710\,\mu m$ but the adsorption rate increased as the particle size decreased. For larger particles, the diffusion limitations are usually more significant and consequently the amount of molecules that reach the internal surface of the biosorbent is small.

3.6. Kinetics of dye removal

The adsorption of both dyes was studied as a function of contact time in order to determine the required time for maximum adsorption. The plots for MB and IC, are shown respectively in Fig. 7(a), (b) and (e), for different initial concentrations.

The results also show that the amount of adsorbed dye, Q_t, increased with the increase of MB initial concentration. For IC the effect was negligible after $300\,mg\,L^{-1}$. The plots in Fig. 7 also indicate that the adsorption is initially fast and then becomes progressively slower with increasing contact time, reaching the equilibrium in less than 30 min. This probably is due to rapid and slow diffusion of dye molecules into the macro- and micropores of the biosorbent. Adsorption processes in liquid–solid interfaces are frequently affected by boundary layer diffusion, or external mass transfer, and intraparticle diffusion. Gong et al. [33] related both diffusion limitations, respectively, to the presence of macropores and micropores in the matrix of biosorbent.

The intraparticle diffusion was investigated using the empirical relationship based on the model of Weber–Morris [34]:

$$q_t = k_i\sqrt{t} + C \quad (6)$$

where k_i is the intraparticle diffusion rate constant ($mol\,g^{-1}\,min^{-1/2}$). A plot of Q_t versus $t^{1/2}$ should be a straight line whose slope gives the value of the diffusion constant. If $C \neq 0$, intraparticle diffusion is not a single rate controlling step [31,33,35].

Fig. 8 shows the plot of intraparticle diffusion for MB and IC onto BNS at initial dye concentration of $1100\,mg\,L^{-1}$, pH = 6.50 and $T = 303$ K.

The linear plots in Fig. 8 did not cross the origin, indicating that although intraparticle diffusion had been significant and that the adsorption of MB and of IC onto BNS surface occurred as a multistep process. Thus, the two linear sections with different slopes were assigned to two intraparticle diffusion steps occurring during the adsorption process, namely, intraparticle diffusion in the macropores and in the micropores. Similar results

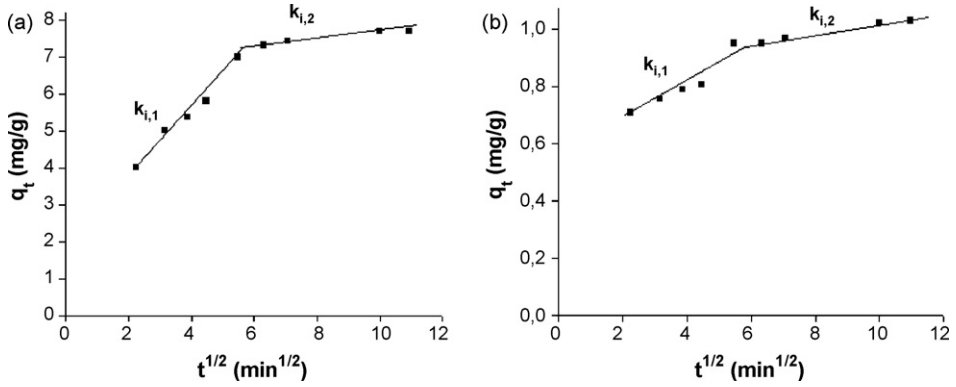

Fig. 8. Intraparticle diffusion plots for (a) methylene blue and (b) índigo carmine onto BNS. $C_0 = 1100\,mg\,L^{-1}$, pH = 6.50, and $T = 303$ K.

Table 3
Intraparticle diffusion constants.

	$k_{i,1}$ (mg g^{-1} min$^{-1/2}$)	R^2	$k_{i,2}$ (mg g^{-1} min$^{-1/2}$)	R^2
Methylene blue	0.88	0.988	0.08	0.96
Indigo carmine	0.07	0.904	0.02	0.98

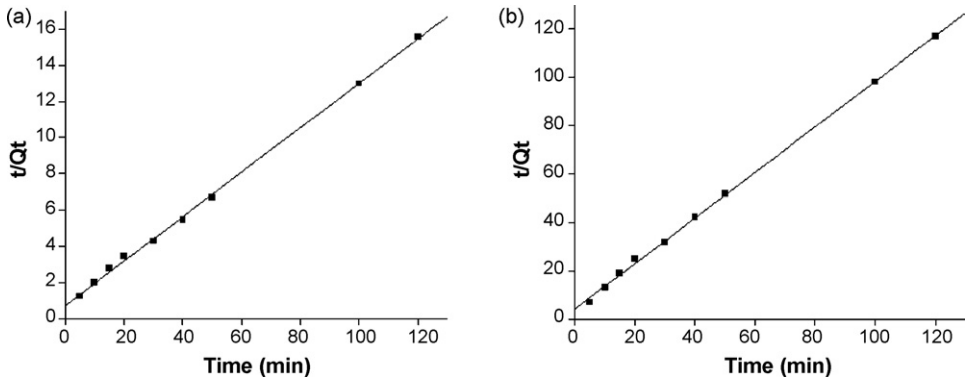

Fig. 9. Pseudo-second order plots for the adsorption of (a) MB and (b) IC at 303 K and initial concentration of 1100 mg L^{-1} and pH = 6.50.

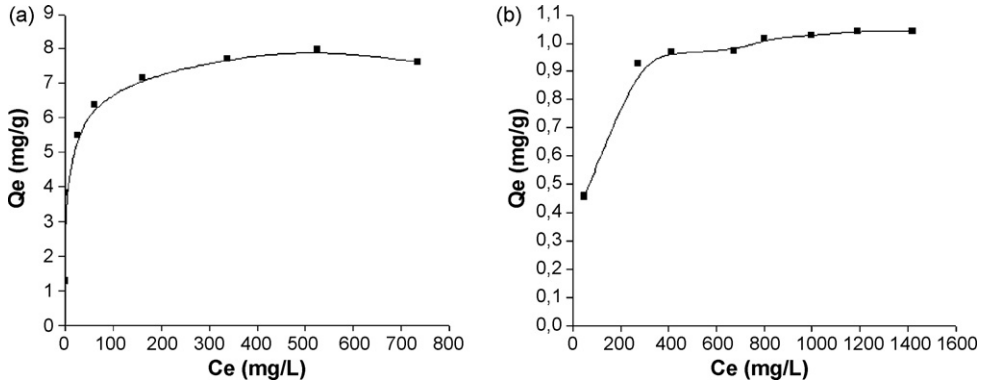

Fig. 10. Langmuir isotherm for MB (a) and IC (b) on BNS at pH = 6.50 and 303 K.

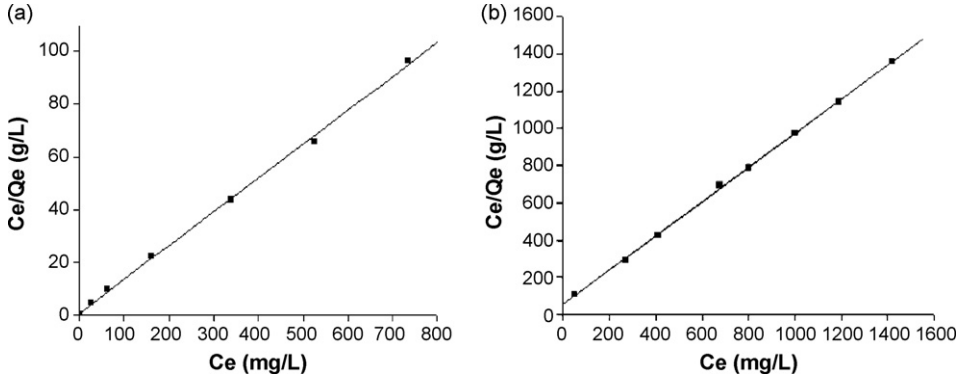

Fig. 11. Langmuir isotherm linear plots for the sorption of MB (a) and IC (b) on BNS at pH = 6.50 and 303 K.

Table 4
Langmuir and Freundlich Isotherm parameters.

Dye	Langmuir parameters			Freundlich parameters		
	Q_{max} (mg g^{-1})	K (L mg^{-1})	R^2[a]	K_F (L mg^{-1})	n	R^2[a]
Methylene blue	7.81	0.15	0.998	0.216	0.876	0.996
Indigo carmine	1.09	0.018	0.999	0.206	4.223	0.931

[a] Linear correlation coefficients.

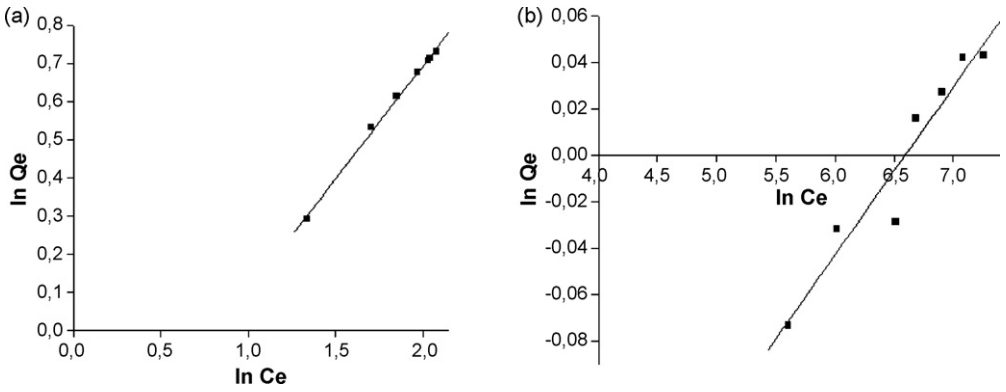

Fig. 12. Plot of linearized Freundlich isotherm for the sorption of methylene blue (a) and indigo carmine (b) on BNS.

have already been reported for dye adsorption onto different biomass materials [31,33,36,37]. The slopes of the linear sections of the plots are shown in Table 3 together with their correlation coefficients. For both dyes $k_{i,2} < k_{i,1}$, indicating that the global adsorption process was controlled by intraparticle diffusion in the micropores of the biosorbent. Moreover, at the same experimental conditions, diffusion limitations are more significant for IC as it is the heavier molecule (MM = 466.36 g mol^{-1}) than MB molecule (MM = 319.85 g mol^{-1}). As previously shown in Table 2, ΔG^0 was more negative for the adsorption of IC than of MB and thus the IC uptake should be more favorable than that of MB, at the same experimental conditions. Contrarily, as shown in Figs. 4, 6 and 8, the IC uptakes were always lower than that of MB, independent of the initial pH, temperature or concentration. Therefore, the IC adsorption onto BNS was thermodynamically favorable but kinetically limited, since only a small amount of dye molecules could slowly reach the microporous surface of the biosorbent.

The kinetics of adsorption of the dyes on BNS was studied by fitting the data to the model of Lagergren first order equation, given by [38,39]:

$$\log_{10}(Q_e - Q_t) = \log_{10} Q_e - \frac{k_{ad}}{2.303} t \quad (7)$$

where Q_e and Q_t are equilibrium uptake and uptake (mg g^{-1}) at time t (min), respectively, and k_{ad} is the adsorption rate constant (min^{-1}) at 28 °C. The obtained linear plots of $\log_{10}(Q_e - Q_t)$ versus t for the studied dyes gave correlation coefficients of about 0.995, suggesting first order adsorption kinetics (graphics not shown). Nevertheless Ho and co-workers [16,17,38–40] found that the pseudo-second order equation fits better the results. According to Kumar [41] the pseudo-second order equation was proposed by Blanchard et al. and has the advantage of predict equilibrium uptake (Q_e) directly from the plot. This equation can be written in different forms. In this work we used the linearized form proposed by Ho et al. [42]:

$$\frac{t}{Q_t} = \frac{1}{k_2 Q_e^2} + \frac{1}{Q_e} t \quad (8)$$

where Q_e and Q_t are equilibrium uptake (mg g^{-1}) and uptake at time t (min) and k_2 is the pseudo-second order rate constant (g mg^{-1} min^{-1}). Fig. 9 shows the plots for pseudo-second order kinetics for both dyes at initial concentration of 1100 mg L^{-1}.

Indeed, the correlation coefficient of about 0.999 indicates that the pseudo-second order equation fits better the results.

The activation energies (E_a) of MB and IC adsorption processes were calculated using the Arrhenius equation [29]:

$$\ln K_a = \ln A - \frac{E_a}{RT} \quad (9)$$

The global activation energies were calculated as 12.40 kJ mol^{-1} and 16.10 kJ mol^{-1} respectively for MB and IC. These values further confirm that rate of adsorption of MB and IC onto BNS is affected by intraparticle diffusion.

3.7. Adsorption isotherms

The adsorption isotherms of MB and IC onto BNS were collected at pH 6.50 and are shown in Fig. 10, as a plot of Q_e (amount of adsorbed dye per mass of adsorbent) versus C_e (equilibrium concentration). Monolayer saturation is attained for both dyes, but the MB uptake is higher than that of IC, as previously discussed.

The adsorption data were treated by Langmuir and Freundlich isotherms, two widely used models. The Langmuir isotherm applies to the adsorption on homogenous surfaces and is based on the assumption that maximum adsorption corresponds to a monolayer coverage on the adsorbent surface. For a single sorbate, Langmuir isotherm is given by:

$$Q_e = \frac{Q_e K C_e}{1 + K C_e} \quad (10)$$

where Q_e is the amount adsorbed per mass of adsorbent (mg g^{-1}), Q_{max} is the monolayer capacity (mg g^{-1}), C_e is the equilibrium concentration (mg L^{-1}) and K is a constant that is related to the energy of adsorption. Although Langmuir isotherm has been developed for gas phase adsorption, Giles et al. [43,44] have demonstrated that this equation can also be useful for liquid phase adsorption.

A linear expression of the Langmuir equation is given by

$$\frac{C_e}{Q_e} = \frac{C_e}{Q_{max}} + \frac{1}{K Q_{max}} \quad (11)$$

Thus, a plot of C_e/Q_e versus C_e gives a straight line of slope $1/Q_{max}$ and intercept $1/KQ_{max}$. Fig. 11 shows the obtained results.

The experimental results fit the linearized Langmuir isotherm for both dyes over the investigated concentration range and the correlation coefficients are as shown in Table 4. These values for the correlation coefficients strongly support the assumption that the adsorption data follows the Langmuir model of sorption. The isotherm constants Q_{max} and K are also shown in Table 4. These results suggest that the adsorption is less favorable for indigo carmine than for methylene blue. The plot in Fig. 11 demonstrates that the Langmuir equation provides an accurate description of the experimental data, which is confirmed by the high values of the correlation coefficients.

The Freundlich isotherm is an empirical equation widely employed to describe solid–liquid adsorption, encompassing the surface heterogeneity. The mathematical expression for the Freundlich isotherm is written as

$$Q_e = K_F C_e^{1/n} \quad (12)$$

Table 5
Comparison of maximum adsorption capacity for MB of some adsorbents.

Adsorbent	Max. capacity ($mg\,g^{-1}$)	pH of adsorption	T (K)	Ref.
BNS	7.81	3–10	303	This work
Marine seaweed	3.42	3–11	300	[45]
Spent tea leaves	300.05	2–11	303	[21]
Coffee husks	90.09	3–11	303	[46]
Pineapple stem	119.05	2–11	303	[47]
Coir pith carbon	5.87	2–11	308	[48]

Table 6
Comparison of maximum adsorption capacity for IC of some adsorbents.

Adsorbent	Max. capacity ($mg\,g^{-1}$)	pH	T (K)	Ref.
Brazil nut shell	1.09	3–11	303	This work
Rice husk ash	29.28	2–10	303	[49]
Bottom ash	0.00017	2–8	303	[50]
De-oiled soya	0.00038	2–8	303	[50]
Chitin	0.0058	Not cited	298	[51]
Chitosan	0.072	Not cited	298	[51]

where Q_e is the amount adsorbed per mass of adsorbent, K_F is the Freundlich constant, C_e is the equilibrium concentration and $1/n$ is interpreted as an heterogeneity factor [29]. A linear form of the Freundlich isotherm can be written as

$$\ln Q_e = \frac{1}{K_F} + \frac{1}{n}\ln C_e \quad (13)$$

Therefore, a plot of $\ln q_e$ versus $\ln C_e$ should be a straight line of slope $1/n$ and intercept $\ln K_F$. Fig. 12 shows the plot of Freundlich isotherm for methylene blue and indigo carmine on BNS.

The values of maximum adsorption of MB and IC onto some alternative adsorbents reported in the current literature are collected in Tables 5 and 6. Although BNS are not among the best adsorbents for MB, they still present higher adsorption capacity than some other adsorbents and may be useful where they are ready available. On the other hand, BNS are among the most efficient adsorbents for indigo carmine (Table 6) at the same pH range.

4. Conclusions

The results above discussed indicated that

- Brazil nut shells (BNS) are useful as low-cost biosorbent for the removal of acid and basic dyes from aqueous solutions.
- The surface of BNS are mostly acid and the amount of surface acid and basic sites corresponded to 7.24 mmol H^+/g and 2.20 mmol OH^-/g, respectively. The mean size of the surface cavities is 7 μm, allowing the dye molecules to penetrate into the lignocellulosic porous structure and interact therein with the surface groups.
- At pH_{PZC} (pH = 6.57) the dye removal from solution by BNS was governed by: (i) polarization effects between the colored ions and the surface sites, leading to physisorbed species due to weak electrostatic forces and (ii) diffusion limitations affecting the kinetic parameters, namely transfer of the dye molecules into the porous structure of the biosorbent.
- Thermodynamic studies showed that, at the experimental conditions, adsorption of methylene blue, a basic dye and of indigo carmine, an acid dye, were spontaneous and exothermic processes, occurring with entropy decrease. ΔH^0 values, namely −5.22 and −3.20 $kJ\,mol^{-1}$, confirmed the physical nature of the adsorption processes, involving weak attractive forces.
- Kinetic studies showed that the adsorption of MB and IC onto BNS followed pseudo-second order kinetics and that the activation energy values further confirmed that the adsorption was affected by intraparticle diffusion.
- MB was more efficiently removed by the adsorption onto BNS than IC. Intraparticle diffusion limitations were more significant for the heavier dye molecules.
- The equilibrium data fitted well in the Langmuir isotherm equation and the maximal uptakes were 7.81 $mg\,g^{-1}$ for MB and 1.09 $mg\,g^{-1}$ for IC, at room temperature.

Acknowledgements

The authors are grateful to FINEP and FAPESB for the financial support for this work.

References

[1] B.T. Tan, T.T. Teng, A.K.M. Omar, Removal of dyes and industrial dye wastes by magnesium chloride, Water Res. 35 (2000) 596–601.
[2] W. Chu, C. Ma, Photodegradation mechanism and rate improvement of chlorinated aromatic dye in non-ionic surfactant solutions, Water Res. 35 (2001) 2453–2459.
[3] Y. Al-Degs, M.A.M. Kharaisher, S.J. Allen, M.N. Ahmad, Effect of carbon surface chemistry on the removal of reactive dyes from textile effluent, Water Res. 34 (2000) 927–935.
[4] H.J. Hao, H. Kim, P.C. Chiang, Decolorization of wastewaters, Crit. Rev. Environ. Sci. Technol. 30 (2000) 449–501.
[5] T. Robinson, G. McMullan, R. Marchant, P. Nigam, Remediation of dyes in textile effluents: a critical review on current treatment technologies with a proposed alternative, Bioresour. Technol. 77 (2001) 247–255.
[6] S.E. Bailey, T.J. Olin, M. Bricka, D.D. Adrian, A review of potentially low cost sorbents for heavy metals, Water Res. 33 (1999) 2469–2479.
[7] C. Namasivayam, N. Kanchana, Waste banana pith as an adsorbent for colour removal from wastewaters, Chemosphere 25 (1992) 1691–1705.
[8] C. Namasivayam, D. Prabha, M. Kumutha, Removal of direct red and acid brilliant blue by adsorption onto banana pith, Bioresour. Technol. 64 (1998) 77–79.
[9] C. Namasivayam, K. Kadirvelu, Coirpith, an agricultural waste by-product for treatment of dyeing wastewater, Bioresour. Technol. 48 (1994) 79–81.
[10] C. Namasivayam, M.D. Kumar, K. Selvi, R.A. Begun, T. Vanathi, R.T. Yamuna, Waste coir pith—a potential biomass for the treatment of dyeing wastewaters, Biomass Bioenergy 21 (2001) 477–483.
[11] B. Chen, C.W. Hui, G. McKay, Film-pore diffusion modelling and contact time optimization for the adsorption of dyestuffs on pith, Chem. Eng. J. 84 (2001) 77–94.
[12] T. Robinson, B. Chandran, P. Nigam, Effect of pre-treatment of three waste residues, wheat straw, corncobs, and barley husks, on dye adsorption, Bioresour. Technol. 85 (2002) 119–124.
[13] A. Shukla, Y.H. Zhang, P. Dubey, J.L. Margrave, S.S. Shukla, The role of sawdust in the removal of unwanted materials from water, J. Hazard. Mater. 95 (2002) 137–152.
[14] T. Robinson, B. Chandran, P. Nigam, Removal of dyes from a synthetic textile dye effluent by biosorption on apple pomace and wheat straw, Water Res. 36 (2002) 2824–2830.
[15] F. Banat, S. Al-Asheh, L. Al-Makhadmeh, Evaluation of the use of raw and activated date pits as potential adsorbents for dye containing waters, Process Biochem. 39 (2003) 193–202.
[16] Y.S. Ho, G. McKay, Sorption of dye from aqueous solution by peat, Chem. Eng. J. 70 (1998) 115–124.

[17] Y.S. Ho, G. McKay, Sorption of dyes and copper ions onto biosorbents, Process Biochem. 38 (2003) 1047–1061.
[18] K.V. Kumar, K. Porkodi, Batch adsorber design for different solution volume/adsorbent mass ratios using the experimental equilibrium data with fixed solution volume/adsorbent mass ratio of malachite green onto orange peel, Dyes Pigment 74 (2007) 590–594.
[19] K.V. Kumar, Optimum sorption isotherm by linear and non-linear methods for malachite green onto lemon peel, Dyes Pigment 74 (2007) 595–597.
[20] S. Chandrasekhar, P.N. Pramada, Rice husk ash as an adsorbent for methylene blue—effect of ashing temperature, Adsorption 12 (2006) 27–43.
[21] B.H. Hameed, Spent tea leaves—a non-conventional and low cost adsorbent for removal of basic dye from aqueous solution, J. Hazard. Mater. 161 (2009) 753–759.
[22] P. Nigam, G. Armour, I.M. Banat, R. Merchant, Physical removal of textile dyes and solid state fermentation of dye adsorbed agricultural residues, Bioresour. Technol. 72 (2000) 219–226.
[23] IBGE, Produção da Extração Vegetal e da Silvicultura 2007, IBGE: Instituto Brasileiro de Geografia e Estatística [Online] 26 de Novembro de 2008 [Citado em: 17 de Março de 2009], http://www.ibge.gov.br/home/presidencia/noticias/noticia_visualiza.php?id_noticia=1270&id_pagina=1.
[24] M. Wainwright, Dyes in the development of drugs and pharmaceuticals, Dyes Pigment 76 (2008) 582–589.
[25] R. Chai, R. Yuan, Y. Chai, C. Ou, S. Cao, X. Li, Amperometric immunosensors based on layer-by-layer assembly of gold nanoparticles and methylene blue on thiourea modified glassy carbon electrode for determination of human chorionic gonadotrophin, Talanta 74 (2008) 1330–1336.
[26] S. Komboonchoo, T. Bechtold, Natural dyeing of wool and hair with índigo carmine (C. I. Natural Blue 2), a renewable resource based blue dye, J. Cleaner Product 17 (2009) 1487–1493.
[27] M. Bozic, V. Kokol, Ecological alternatives to the reduction and oxidation processes in dyeing with vat and sulphur dyes, Dyes Pigment 76 (2008) 299–309.
[28] A.P. Vieira, S.A.A. Santana, C.W.B. Bezerra, H.A.S. Silva, J.A.P. Chaves, J.C.P. de Melo, E.C. da Silva Filho, C. Airoldi, Kinetics and thermodynamics of textile dye adsorption from aqueous solutions using babassu coconut mesocarp, J. Hazard. Mater. 166 (2009) 1272–1278.
[29] S.L.C. Ferreira, H.M.C. Andrade, H.C. dos Santos, Characterization and determination of the thermodynamic and kinetic properties of the adsorption of the molybdenum(VI)-calmagite complex onto activated carbon, J. Colloid Interface Sci. 270 (2004) 276–280.
[30] S.J. Allen, G. McKay, J.F. Porter, Adsorption isotherm models for basic dye adsorption by peat in single and binary component systems, J. Colloid Interface Sci. 280 (2004) 322–333.
[31] M. Dogan, H. Abak, M. Alkan, Adsorption of methylene blue onto hazelnut shell: kinetics, mechanism and activation parameters, J. Hazard. Mater. 164 (2009) 172–181.
[32] C.H. Weng, Y.T. Lin, T.W. Tzeng, Removal of methylene blue from aqueous solution by adsorption onto pineapple leaf powder, J. Hazard. Mater. 170 (2009) 417–424.
[33] R.M. Gong, S.X. Zhu, D.M. Zhang, J. Chen, S.J. Ni, R. Guan, Adsorption behavior of cationic dyes on citric acid esterified wheat straw: kinetic and thermodynamic profile, Desalination 230 (2008) 220–228.
[34] W.J. Weber, J.C. Morris, Kinetics of adsorption on carbon from solution, J. Sanit. Eng. Div. Am. Soc. Civ. Eng. 89 (1963) 31–60.
[35] Y.S. Ho, Removal of copper ions from aqueous solution by tree fern, Water Res. 37 (2003) 2323–2330.
[36] M. Dogan, Y. Ozdemir, M. Alkan, Adsorption kinetics and mechanism of cationic methyl violet and methylene blue dyes onto sepiolite, Dyes Pigments 75 (2007) 701–713.
[37] Q.Y. Sun, L.Z. Yang, The adsorption of basic dyes from aqueous solution on modified peat-resin particle, Water Res. 37 (2003) 1535–1544.
[38] Y.S. Ho, C.C. Chiang, Sorption studies of acid dye by mixed sorbents, Adsorption 7 (2001) 139–147.
[39] Y.S. Ho, C.C. Chiang, Y.C. Hsu, Sorption kinetics for dye removal from aqueous solution using activated clay, Sep. Sci. Technol. 36 (2001) 2437–2488.
[40] Y.S. Ho, Pseudo-isotherms using a second order kinetic expression constant, Adsorption 10 (2004) 151–158.
[41] K.V. Kumar, A note on the comments by Dr. Y.S. Ho on 'Remediation of soil contaminated with the heavy metal (Cd^{2+})', J. Hazard. Mater. 136 (2006) 993–994.
[42] Y.S. Ho, G. McKay, Kinetic models for the sorption of dye from aqueous solution by wood, Process Safe. Environ. Protect. 76B (1998) 183–191.
[43] C.H. Giles, D. Smith, A. Huitison, A general treatment and classification of the solute adsorption isotherm. I. Theoretical, J. Colloid Interface Sci. 47 (1974) 755–765.
[44] C.H. Giles, A.P. D'Silva, I.A. Easton, A general treatment of the solute adsorption isotherm. Part II. Experimental interpretation, J. Colloid Interface Sci. 47 (1974) 766–778.
[45] S. Cengiz, L. Cavas, Removal of methylene blue by invasive marine seaweed: *Caulerpa racemosa* var. cylindracea, Bioresour. Technol. 99 (2008) 2357–2363.
[46] L.S. Oliveira, A.S. Franca, T.M. Alves, S.D.F. Rocha, Evaluation of untreated coffee husks as potential biosorbents for treatment of dye contaminated waters, J. Hazard. Mater. 155 (2008) 507–512.
[47] B.H. Hameed, R.R. Krishni, S.A. Sata, A novel agricultural waste adsorbent for the removal of cationic dye from aqueous solutions, J. Hazard. Mater. 162 (2009) 305–311.
[48] D. Kavitha, C. Namasivayam, Experimental and kinetic studies on methylene blue adsorption by coir pith carbon, Bioresour. Technol. 98 (2007) 14–21.
[49] U.R. Lakshmi, V.C. Srivastava, I.D. Mall, D.H. Lataye, Rice husk ash as an effective adsorbent: evaluation of adsorptive characteristics for indigo carmine dye, J. Environ. Manage. 90 (2009) 710–720.
[50] A. Mittal, J. Mittal, L. Kurup, Batch and bulk removal of hazardous dye indigo carmine, from wastewater through adsorption, J. Hazard. Mater. 137 (2006) 591–602.
[51] A.G.S. Prado, J.D. Torres, E.A. Faria, S.C.L. Dias, Comparative adsorption studies of indigo carmine dye on chitin and chitosan, J. Colloid Interface Sci. 277 (2004) 43–47.